Investigation of Load-Transfer Mechanisms in Geotechnical Earth Structures with Thin Fill Platforms Reinforced by Rigid Inclusions

B. Chevalier[1]; P. Villard[2]; and G. Combe[3]

Abstract: The reinforcement of soft soils by rigid inclusions is a practical and economical technique for wide-span buildings and the foundations of embankments. This method consists of placing a granular layer at the top of the network of piles to reduce vertical load on the supporting soil and vertical settlement of the upper structure. The study focuses on the modeling of load-transfer mechanisms occurring in the reinforced structure located over the network of piles with a coupling between the finite-element method (geosynthetic sheets) and discrete element method (granular layer; concrete slab in some cases). The importance of granular layer thickness to increase load-transfer intensity and to reduce vertical settlement was observed. However, without a basal geosynthetic sheet, the compressibility of soft soil has a great influence on the mechanisms. A method predicting the intensity of load transfers was proposed, based on Carlsson's solution. The main parameters concerned are the geometry of the work and the peak and residual friction angles of the granular layer. **DOI: 10.1061/(ASCE)GM.1943-5622.0000083.** © *2011 American Society of Civil Engineers.*

CE Database subject headings: Soil structures; Fills; Piles; Geosynthetics; Discrete elements; Finite element method; Coupling; Load transfer; Granular media.

Author keywords: Soil reinforcement; Rigid inclusions; Piles; Basal geosynthetic; Discrete element method; Finite-element method; Coupling; Load transfer; Granular material.

Introduction

Civil engineering works constructed on very soft soils are potentially subjected to considerable absolute or differential settlement. These displacements must be limited to admissible values to maintain the stability, structural integrity, and durability of the civil engineering structures concerned. For large-scale works in particular (roads, highways, railways, and industrial buildings), the use of traditional foundation techniques can rapidly lead to prohibitive costs and delays. Over the last few decades, the rigid inclusions technique has provided an interesting alternative to traditional methods of reinforcement.

This technique is based on the use of a network of piles, a granular load-transfer layer located over the piles, and in some cases, geosynthetic reinforcement inserted in the middle or at the base of the granular layer (a geogrid or geosynthetic sheet).

[1]Ph.D. Student, Grenoble Universités, Laboratoire Sols, Solides, Structures—Risques UMR CNRS/UJF/INPG (3S-R), Domaine Universitaire, BP 53, F-38041 Grenoble Cedex 9, France (corresponding author). E-mail: bastien_chevalier@yahoo.fr

[2]Professor, Grenoble Universités, Laboratoire Sols, Solides, Structures—Risques UMR CNRS/UJF/INPG (3S-R), Domaine Universitaire, BP 53, F-38041 Grenoble Cedex 9, France. E-mail: pascal.villard@ujf-grenoble.fr

[3]Assistant Professor, Grenoble Universités, Laboratoire Sols, Solides, Structures—Risques UMR CNRS/UJF/INPG (3S-R), Domaine Universitaire, BP 53, F-38041 Grenoble Cedex 9, France. E-mail: gael.combe@ujf-grenoble.fr

Note. This manuscript was submitted on October 28, 2009; approved on August 4, 2010; published online on August 6, 2010. Discussion period open until November 1, 2011; separate discussions must be submitted for individual papers. This paper is part of the ***International Journal of Geomechanics***, Vol. 11, No. 3, June 1, 2011. ©ASCE, ISSN 1532-3641/2011/3-239–250/$25.00.

The primary interest of this procedure is to increase the part of the load redirected to the rigid network of piles to reduce the vertical load acting on both the soft soil and surface settlement. For building applications, which require very low differential settlement, a rigid slab is commonly used.

Such mechanisms, i.e., those involving the use of a granular layer, geosynthetic reinforcement, or a concrete slab, are sophisticated and their description by means of an analytical design scheme remains problematic. Current design methods are restricted to the description of the load-transfer mechanisms involved in the granular layer (British Standards Institution 1995; Øiseth and Busklein 2001; Deutsche Gesellschaft für Geotechnik 2004). They can be divided into three categories. The first category considers that the mechanisms inside the granular layer are similar to those described by Terzaghi (1943). In this case, the granular layer can be divided into two areas: the fixed parts located exactly above the piles, and the other parts that slide between the fixed parts and thus induce friction and load-transfer toward the inclusions (Combarieu 1988, 1990; Russel and Pierpoint 1997). This method gave rise to the British Standard 8006 (British Standards Institution 1995). The second assumes a zone of influence over each pile from which the load transfers can be obtained (Carlsson 1987; Svano et al. 2000; Øiseth and Busklein 2001). Finally, the third category considers that an arching effect occurs between two adjacent piles and calculates the load-transfer depending on this preassumed shape of the arch (Hewlett and Randolph 1988; Kempfert 1997; Deutsche Gesellschaft für Geotechnik 2004). These different approaches are still subject to discussions and improvements, particularly when geosynthetics are used (Yun-Min et al. 2008; Abusharar et al. 2009).

To establish specific design or execution regulations dedicated to the technique of rigid inclusions, a national project, called Amélioration des Sols par Inclusions Rigides (A.S.I.Ri), was

carried out in France to investigate the mechanisms involved in such works.

The aim of this project was to give a technical and cost-effective response to the soft soil reinforcement problem with rigid piles that satisfy industrial needs. To lessen costs (of labor and of materials supply) and to limit environmental impact, the project work focused on thin granular platforms with 0.5 to 1.0 m thickness and low coverage rates of the piles between 2 and 5% (the coverage rate is the ratio of the area of the pile heads to the total area). These values are rather smaller than the recommendations of classical design methods: British Standard BS8006 (British Standards Institution 1995) and Hewlett and Randolph (1988) recommend a thickness of granular fill above piles at least 0.7 to 1.4 times the spacing of piles, and Han and Gabr (2002) recommend a coverage rate of piles ranging from 10 to 20%.

As part of this project, a numerical study was carried out using an original numerical tool based on a coupling between the discrete and finite-element methods. This study is focused on the mechanisms of load-transfer toward the piles network by means of either the granular layer, geosynthetic sheet, or rigid slab.

The numerical model and special coupling between finite and discrete element methods, used for the modeling of such structures, are described in the first section. The second part presents the typical geometry of the cases studied and the numerical procedures of the simulations carried out. Finally, three different configurations of reinforcement were studied, taking into account a granular layer, a foundation slab, or a basal geosynthetic sheet.

Numerical Model

A coupling of the discrete element method (DEM) and the finite-element method (FEM) was used for modeling the granular material and geosynthetic sheets, respectively. This coupling was validated (Villard et al. 2009) by comparing numerical analyses and full-scale field experiments.

The DEM part of the modeling was based on molecular dynamics (Cundall and Strack 1979). The granular material is modeled with rigid particles that interact through contact forces. The time-iterative process consists of successively applying Newton's second law of motion on each particle, updating particle positions and contact points, computing contact forces, and updating the force balance on each particle. An explicit leapfrog scheme is used to integrate the equations of motion (Allen and Tildesley 1994). The normal component of contact forces between particles is deduced from linear normal contact laws

$$f_n = k_n h_{ij} \tag{1}$$

where k_n = normal stiffness of the contact and h_{ij} = overlap between the two particles i and j in contact.

No attraction forces between the particles were considered (the contacts are cohesionless). The tangential component of the contact force is calculated with the expression proposed by Cundall and Strack (1979) and is limited by a Coulomb friction criterion of coefficient μ:

$$\frac{df_t}{d\delta u_t} = k_t \quad \text{and} \quad |f_t| \le \mu f_n \tag{2}$$

where k_t = tangential stiffness of the contact; δu_t = incremental tangential displacement between the two particles. Combe (2002) showed in static conditions that considering a ratio k_t/k_n between 0.5 and 1 does not influence the results of modeling. In addition, Schäfer (1996) recommended setting the ratio k_t/k_n to 0.75 in dynamic conditions. In the numerical simulations under discussion in this paper, the ratio k_t/k_n was fixed at a value of 0.75.

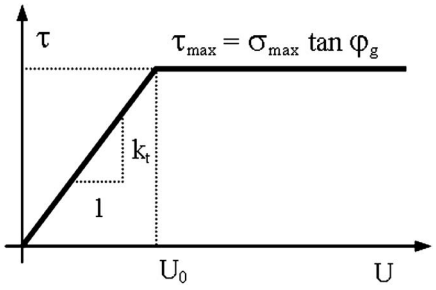

Fig. 1. Interaction law between soil particles and sheet elements

The finite-element model uses three-node triangular elements connected to one other to describe the fibrous structure of the geosynthetic sheets (Villard and Giraud 1998). The tensile and membrane behaviors of the sheet are rigorously reproduced on the basis of a mathematical description in large strains. The global mechanical behavior of the geosynthetic sheet depends on the tensile stiffness J associated to each direction of the fibers. The tensile force T in a given direction of fiber depends on the deformation ε and the stiffness J of the fiber in the considered direction:

$$T = J\varepsilon \tag{3}$$

Laboratory and field tests on full-scale works have successfully validated this finite element modeling of geosynthetic sheets (Villard et al. 2000; Gourc and Villard 2000).

The interaction between discrete and finite elements is handled by the contacts between the particles and the triangular elements. Normal and tangential linear contact laws are considered. The role of the normal stiffness of these contacts is only to prevent the particles from passing through sheet elements. The tangential contact force is regulated by an elastic-plastic behavior commonly used in numerical approaches (Villard 1996; Reddy et al. 1996; Villard et al. 2009) and limited by a Coulomb friction criterion (Fig. 1). The relative displacement between the particles and the geosynthetic sheet, necessary for the friction interaction to be fully developed, was called U_0.

Geometry and Characteristics of the Numerical Simulations

The numerical analysis was based on the geometry and characteristics of materials used in full-scale experimental tests (Briançon 2007) performed in France within the framework of the A.S.I.Ri Project.

A granular layer of thickness h_m is placed on a soft soil reinforced with a network of rigid piles spaced out in a square mesh. Owing to symmetry conditions, the analysis was performed on a square elementary cell of 2.50×2.50 m^2 (Fig. 2). Each pile has a square section of 0.37×0.37 m^2. Thus, the covering rate, which is the ratio of the area of the pile head to the area of the elementary cell, represents 2.19%.

Load-Transfer Layer

The numerical load-transfer layers consist of an assembly of particles, generated randomly in a polygonal area at the minimal porosity of 0.355, using the radius expansion with decrease of friction (REDF) process (Chareyre and Villard 2005). Two thicknesses of the granular layer were considered: a load-transfer layer 0.5-m-high made up of 16,000 particles and another 1-m-high made up of

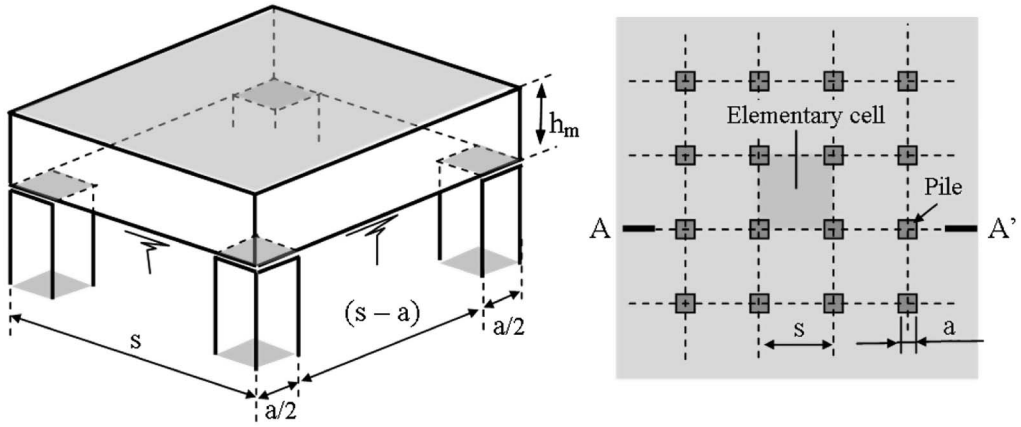

Fig. 2. Geometry of the full-scale experimental tests

32,000 particles (Fig. 3). Each particle is composed of a perfectly rigid assembly of two overlapped spheres of diameter d. The distance between the centers of the two spheres of one particle is equal to $0.95d$. The diameters d of the spheres are equally distributed between 0.01 and 0.04 m.

The contact parameters of the granular assembly, shown in Table 1, were chosen to reproduce the experimental shear strength levels that corresponded to commonly used granular materials for soft soil reinforcement works. Fig. 4 shows the numerical response of a sample of 8,000 particles in a triaxial test with a 50 kPa confining pressure, corresponding to the average stress level applied during loading to the granular material sited over the piles.

The numerical response of the sample of 8,000 particles to the triaxial compression test gave an initial tangent Young modulus equal to 257 MPa and a corresponding Poisson's ratio equal to 0.08. The small value of the Poisson ratio is classically observed with high coordination numbers and high Young moduli (Kuwano and Jardine 2002; Chevalier et al. 2007).

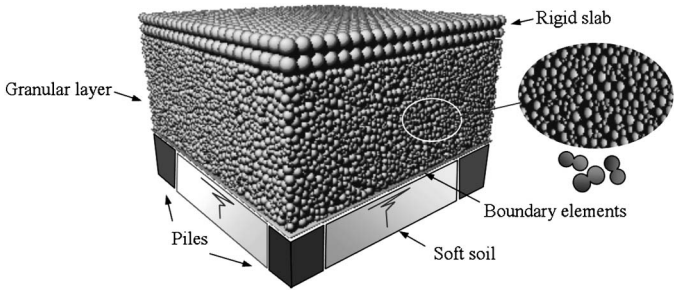

Fig. 3. View of the numerical model ($h_m = 1$ m)

Table 1. Micro and Macro Mechanical Parameters of the Numerical Granular Material

Average normal stiffness	k_n	1.3×10^7 kN/m
Ratio of tangential to normal stiffness	k_t/k_n	0.75
Friction coefficient	$\tan\mu$	0.577
Young modulus	E_0	257 MPa
Poisson ratio	ν	0.08
Peak friction angle	φ_p	44.8°
Residual friction angle	φ_r	30.1°
Dry apparent density	γ_d	17.7 kN/m^3

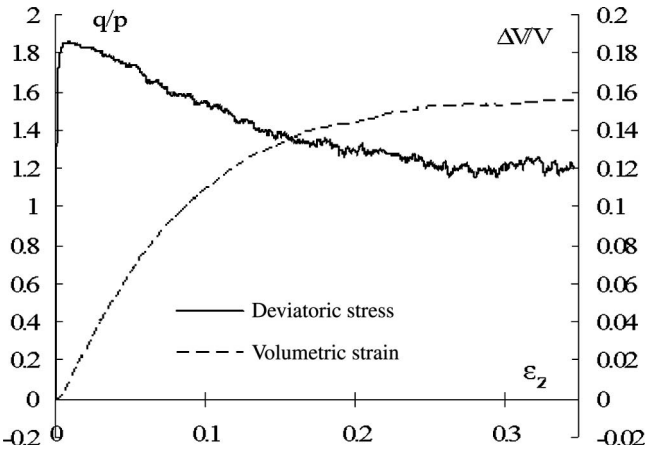

Fig. 4. Numerical curves of the triaxial test, performed on the granular material under a 50 kPa confining pressure

Foundation Slab

The slab, usually considered for building applications, was modeled with DEM using an assembly of spheres with the same diameter uniformly arranged into two layers (Fig. 3). These spheres are bound with elastic and unbreakable links of parameters k_n and k_t. The bending moment in the slab is deduced from the forces within the upper and lower layers. Considering the analytical solutions of bending a simple supported beam, the normal contact stiffness k_n was determined. The tangential contact stiffness k_t was set to fit the deflection behavior of the slab embedded on its four borders (Chevalier 2008). Bending tests were modeled to validate these values. To guarantee the cohesion of the slab, a high attraction force was taken into account between the two layers of spheres. A precise description of the slab is not necessary here, because the determination of the forces and bending moments that occurred in the slab is not the purpose of this paper: the main objective is to sufficiently reproduce the bending behavior of the slab.

Geosynthetic Sheets

The geosynthetic sheet was modeled by an assembly of triangular elements connected to one other. It was assumed that the sheet was reinforced by two perpendicular directions of fibers with tensile stiffness J, depending on the case studied: $J = 750$ kN/m or $J = 1{,}500$ kN/m.

The macroscopic behavior of contact among soil particles and geosynthetic sheets is characterized through experimental

laboratory tests (frictional or pull-out tests). The angle of friction measured between the soils and the geosynthetics sheets is $\varphi_g = 30°$. The tangential contact stiffness k_{tg} (Fig. 1) between granular particles and triangular elements is deduced from the ratio of average normal stress at the interface σ_{max} to the relative displacement U_0 needed to fully mobilize the friction (Pasqualini 1993; Gilbert 1996). The normal stress at the interface σ_{max} was attributable to the self-weight of the granular layer, and the relative displacement U_0 was considered equal to a few millimeters.

Soft Soil and Boundary Conditions

The purpose of this study focuses on the load-transfer occurring in the granular layer. Therefore, the mechanisms occurring among the soft soil and the network of piles were not considered. Consequently, the soft soil was modeled in a simplified way by vertical springs (linear Winkler model). The stiffness K_c of the springs depends on the compressibility of the soft soil and links the settlement δ of the soft soil to the vertical stress σ_v applied:

$$\sigma_v = K_c \delta \tag{4}$$

K_c is given in MPa/m and represents an equivalent height h_c of soft soil with an oedometric modulus E_{oed}:

$$K_c = \frac{E_{oed}}{h_c} \tag{5}$$

Four values of K_c were considered to determine its influence on the load transfers: $K_c = \{0.25; 0.50; 0.75; 1.00\}$ MPa/m.

The boundary elements (Fig. 3) between the soft soil and the granular layer were finite elements similar to those used for modeling the geosynthetic sheets, but with a negligible value of the tensile stiffness J. The boundary elements over the pile heads were fixed in the three directions of space. To introduce the symmetry, four frictionless vertical planes were used around the elementary cell.

Load Process

Gravity forces were applied on the load-transfer layer while the soft soil was maintained inactive. After that, the Winkler springs were released. Once a state of equilibrium was reached, an overload was applied by increments above the granular layer. The following load increment was applied only once an equilibrium state was reached. The equilibrium criterion used was calculated with the resulting vertical forces F_z on soft soil and piles with the following condition:

$$\left|1 - \frac{F_z}{W + Q}\right| \leq 10^{-3} \tag{6}$$

where W = weight of the load-transfer layer (including the weight of the slab, if any) and Q = actual overload on the granular layer. The successive values of the uniform vertical overload stresses q were: 12.8, 25.5, 46.8, and 68 kPa. The total stress q_t resulting from the self weight of the granular layer (including the concrete slab, if any) and the overload q can be written

$$q_t = \gamma h_m + q \tag{7}$$

Load-Transfer Mechanisms

Two common applications of soft soil reinforcement with rigid piles are reinforcement under buildings and embankments (basically, road or railway embankments). The main differences between these are, the deformation tolerance of the upper structure and the boundary conditions involved by the possible use of a rigid slab. The mechanisms resulting from these two applications are consequently fundamentally different, and are presented here in distinct sections.

Application to Reinforcement Under Embankments

Typical Results of the Load-Transfer Mechanisms

The load-transfer mechanisms result from the differential settlements produced by the contraction of the soft soil. To analyze these phenomena, basic numerical simulations were carried out under the following conditions:

1. Height of granular layer: $h_m = 0.5$ or 1.0 m;
2. Stiffness of the soft soil: $K_c = 0.75$ MPa/m; and
3. No geosynthetic reinforcement.

The global load-transfer mechanisms acting inside the granular layer are quantified with the efficiency (E) defined by the ratio of the load applied on one pile F_p to the total vertical load applied on an elementary cell $W + Q$:

$$E = \frac{F_p}{W + Q} \tag{8}$$

Without transfer of load, the efficiency E tends to the value of the covering rate: 2.19% in this case. The ability of the load-transfer layer to redirect the overload Q to the piles can be given by the following ratio G:

$$G = \frac{\Delta F_p}{\Delta Q} \tag{9}$$

where ΔF_P = increase of the load consecutively redirected to the piles with the application of an overload ΔQ.

The values of E and G versus the total load q_t are given in Fig. 5 and 6 for the granular layer heights of $h_m = 0.5$ m and $h_m = 1.0$ m. Fig. 5 shows that the efficiency E increases with the total load applied q_t, and reaches a threshold value of approximately 30% for $h_m = 0.5$ m and 65% for $h_m = 1.0$ m. These threshold values are much higher than the covering rate value of 2.19%. The results in Fig. 6 show that the ability of the layer to redirect the overload to the piles is relatively constant, approximately 35% for $h_m = 0.5$ m and 75% for $h_m = 1.0$ m. Consequently, Fig. 7 shows that for a fixed value of the total load q_t, an increase in the height of the granular layer involves a reduction of the maximum vertical settlement of the soft soil δ.

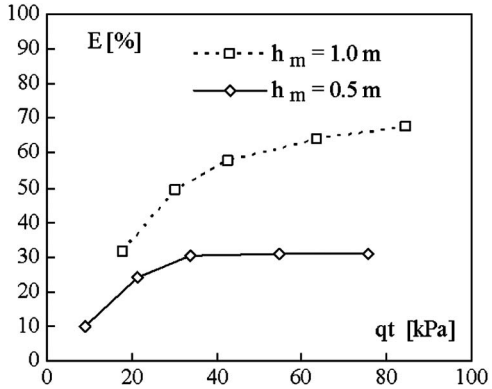

Fig. 5. Efficiency of the granular layer

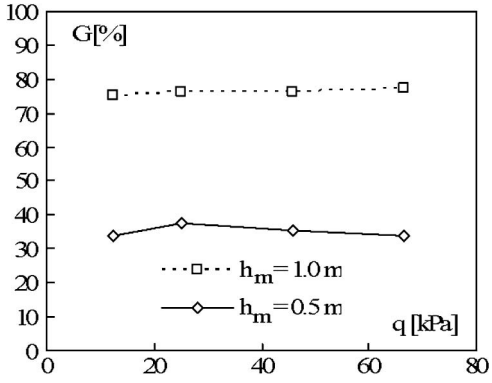

Fig. 6. Ability of the load-transfer layer to redirect the upper overload to the piles

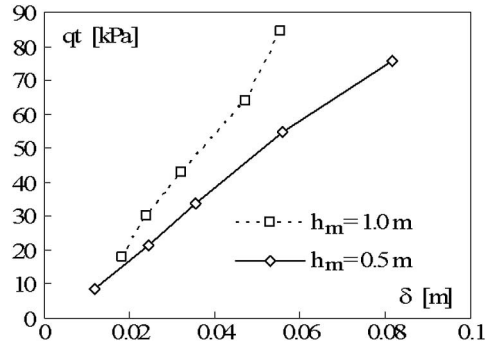

Fig. 7. Maximum vertical settlements of the soft soil

Proposal of an Analytical Formulation of the Load-Transfer Mechanisms

To describe the mechanisms occurring in the load-transfer layer, the intensities of the vertical displacements of the granular particles were represented in a vertical cross-section (section A–A' in Fig. 2) for the different phases of the loading process for $h_m = 0.5$ m in Fig. 8 and for $h_m = 1.0$ m in Fig. 9.

The pattern observed in the displacement intensity distribution shows two different areas in the granular layer: the first, located above the piles, in which the granular particles have very small displacements; and the second, above the soft soil, in which the granular particles move with the soft soil. This geometry is reminiscent of the solution of Carlsson (1987), in which part of the load is transferred to the piles through a specific area located just above the piles and presenting the shape of an inverted pyramid (Fig. 10). Following Carlsson's recommendation, the pyramid area is characterized by an angle θ equal to 15°, whatever the granular layer mechanical characteristics.

The value of the efficiency E can be deduced from this assumption depending on the angle θ, the overload q, the distance between piles s, the size of the pile head a, the height h_m, and the density of the layer γ_m.

The part W_p of the weight of the granular layer redirected to the piles can be written

$$W_p = \frac{\gamma}{6\tan\theta}((a + 2h_m\tan\theta)^3 - a^3) \quad \text{for } h_m \le h^* = \frac{s-a}{2\tan\theta} \tag{10}$$

When $h_m > h^*$, the load-transfer zones located over each pile meet, and therefore, the load-transfer layer located above h_m acts as an overload.

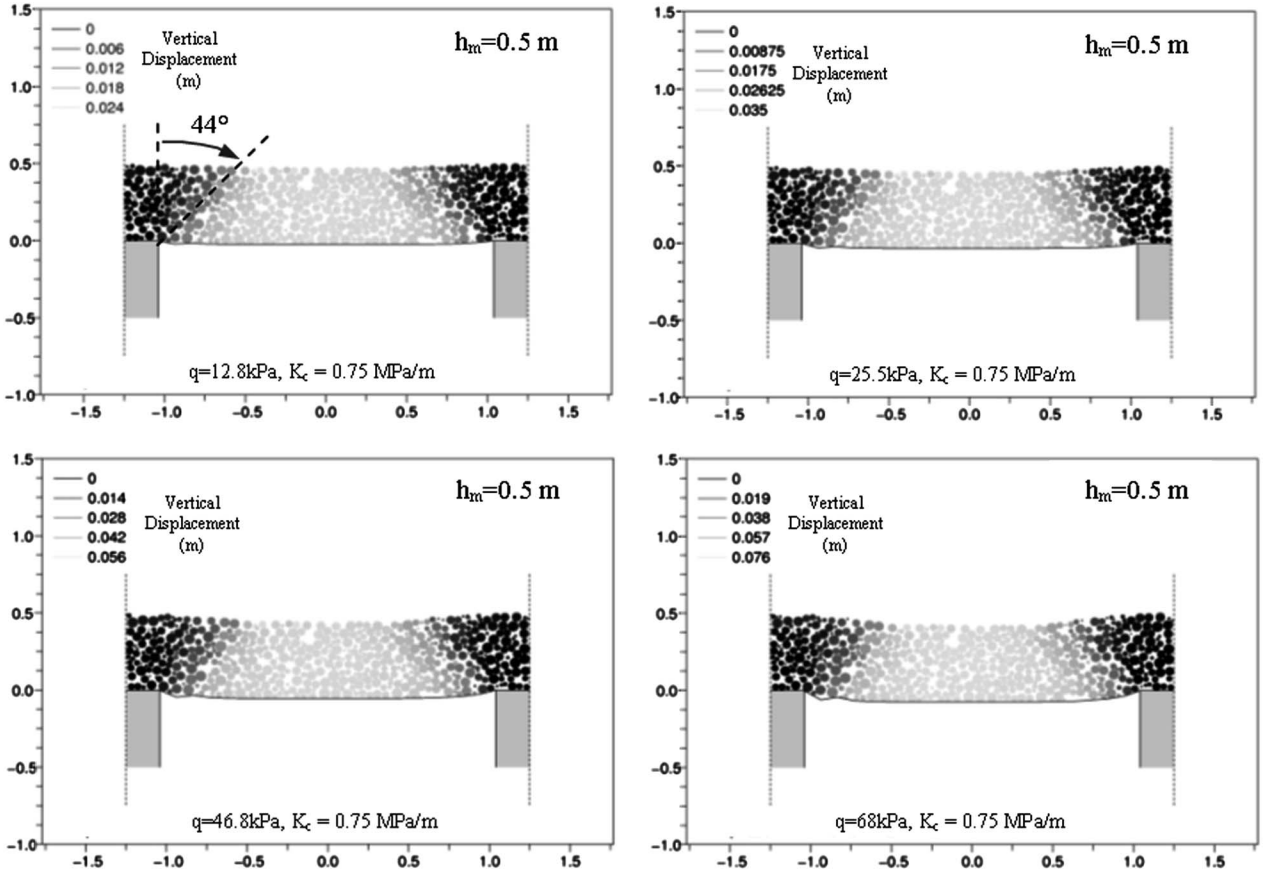

Fig. 8. Particle displacements in a vertical cross-section for $h_m = 0.5$ m, $K_c = 0.75$ MPa/m, and each overload stage

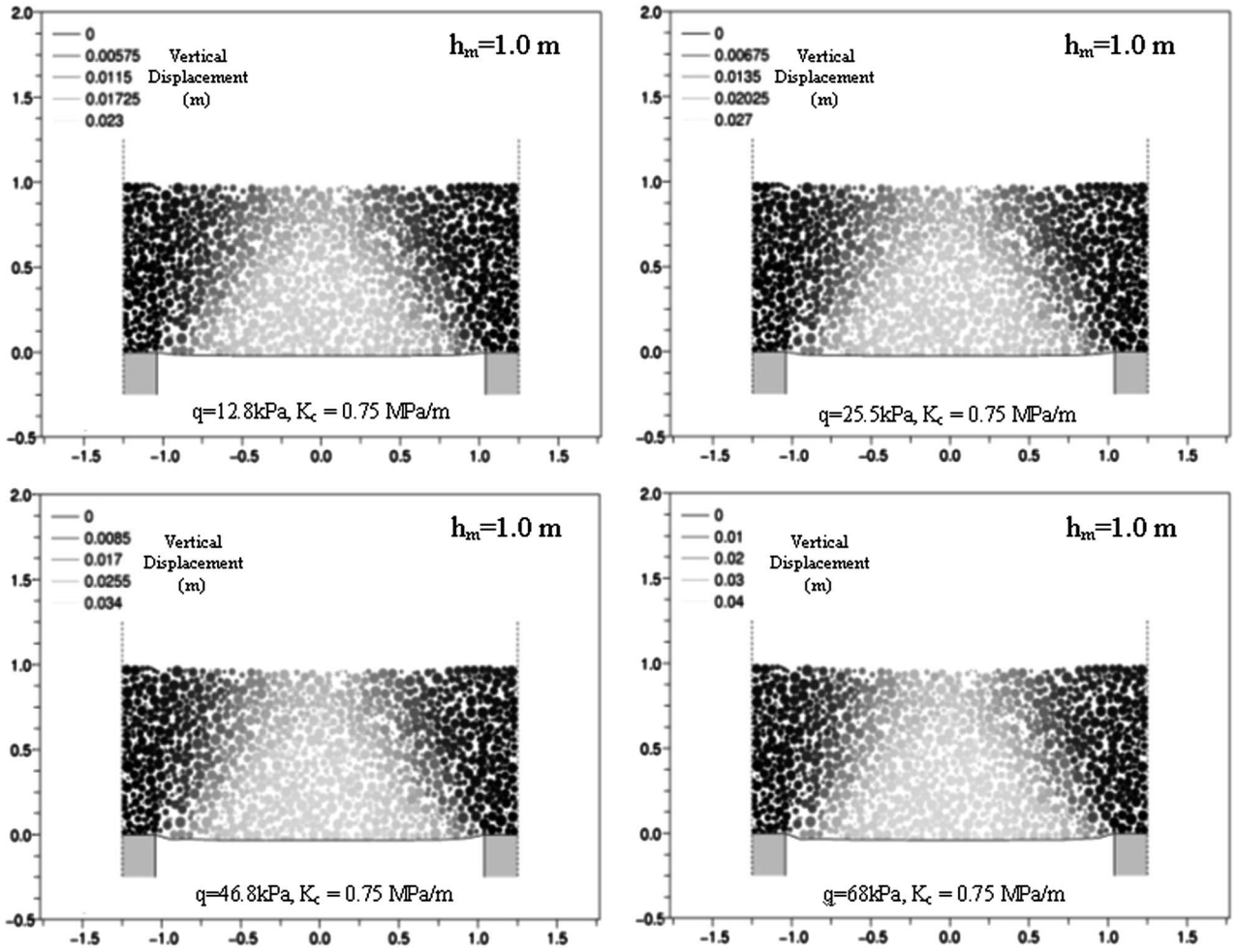

Fig. 9. Particle displacements in a vertical cross-section for $h_m = 1.0$ m, $K_c = 0.75$ MPa/m, and each overload stage

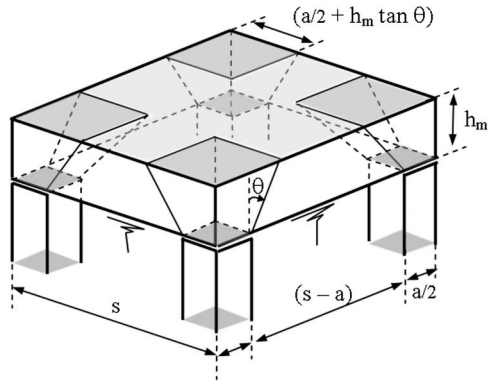

Fig. 10. Carlsson's description of the load-transfer areas with an inverted pyramid shape

The part of the overload q redirected to the piles by the load-transfer zone is assumed to act on square areas (Fig. 10). This can be written

$$Q_p = q(a + 2h_m \tan\theta)^2 \quad \text{for } h_m \le h^* = \frac{s-a}{2\tan\theta} \tag{11}$$

Consequently, a prediction of the efficiency E' is given by

$$E' = \frac{W_p + Q_p}{s^2(\gamma h_m + q)} \tag{12}$$

If the overload greatly increases, the value of the efficiency E'_∞ tends to a value that depends only on θ and on the geometric characteristics

$$E'_\infty = \frac{(a + 2h_m \tan\theta)^2}{s^2} \tag{13}$$

Contrary to the Carlsson proposal, the angle θ obtained in the numerical study is equal to 45°, close to the value of the peak friction angle of the granular material. Fig. 11 shows a comparison of the efficiencies E obtained with the numerical analysis and the predictions E' using Eq. (12) with $\theta = \varphi_p = 45°$. To estimate the influence of the value of θ on the prediction, the curves for $\theta = \varphi_p + 3°$ and $\theta = \varphi_p - 3°$ are shown in the same figure.

Fig. 11 shows that the prediction E' slightly underestimates the numerical results E when $h_m = 0.5$ m, whereas E' overestimates E for $h_m = 1.0$ m. The assumption of an inverted pyramid shape is no doubt an approximation of the real phenomenon; nevertheless, the evolution of the efficiency as the load q_t increases is correctly reproduced, as is the influence of the height of the load-transfer layer. However, a small variation in the angle θ leads to a relatively large variation of the predicted value of E.

Influence of Soft Soil Stiffness on the Load-Transfer Mechanisms

The analytical formulation of Eq. (12) for the load-transfer mechanisms was compared only for the value of the soft soil stiffness $K_c = 0.75$ MPa/m. Other numerical simulations were carried

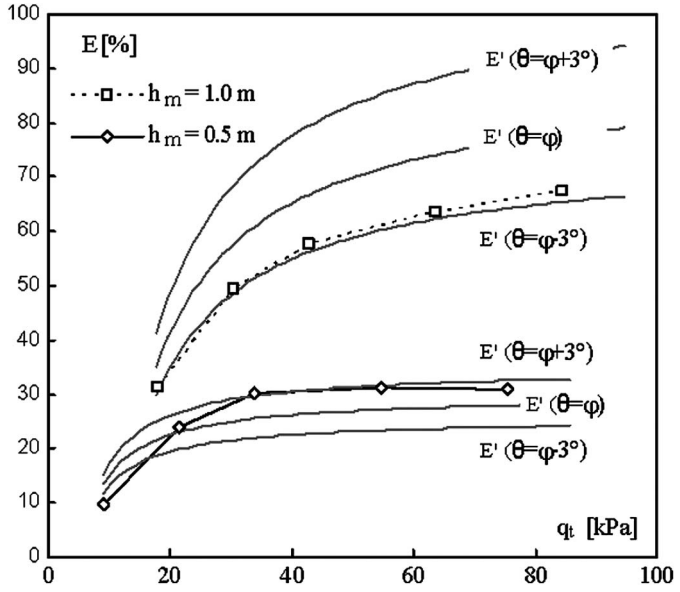

Fig. 11. Comparison of the efficiency E obtained from numerical modelling and the analytical prediction E', for $h_m = 0.5$ m and $h_m = 1.0$ m

out for other values of K_c, ranging from 0.25 to 1.00 MPa/m in cases of $h_m = 0.5$ m and $h_m = 1.0$ m. The influence on load transfers of the compressibility of soft soil and consequently its settlements is given in Figs. 12 and 13.

These figures show that the coefficient G depends on the vertical settlement of the soft soil δ, and is strongly affected by low values of the soft soil stiffness. For low values of settlement, the efficiency of the granular layer depends essentially on the height of the granular layer, independent of K_c.

The tendency of the load-transfer amplitude to decrease as the settlement at the base of the granular layer increases is similar to that observed in trap-door tests (Chevalier et al. 2008). These works show that the amplitudes of the load transfers, for low and high values of the trap-door displacement, were linked to the peak and residual friction angles, respectively. To discover whether such mechanisms are still valid in the case of the rigid inclusions technique, the distribution of the vertical displacements of particles for large settlements is presented in Fig. 14.

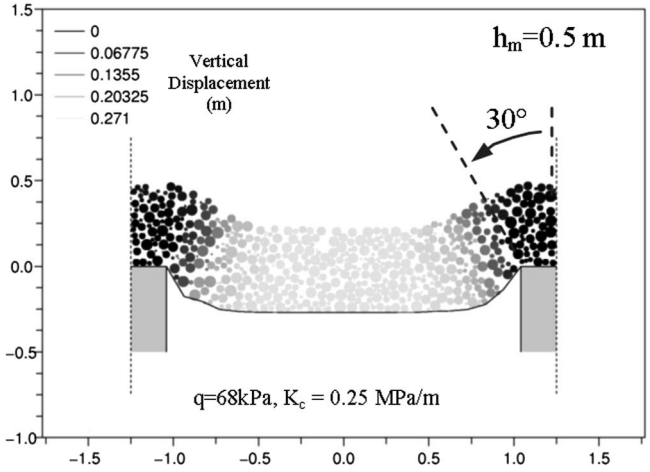

Fig. 14. Particle displacements in vertical cross-section for low values of soft soil stiffness ($h_m = 0.5$ m and $K_c = 0.25$ MPa/m)

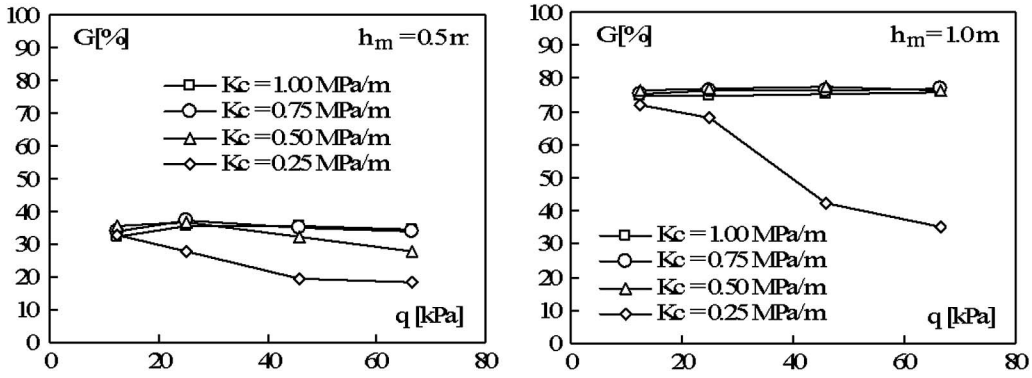

Fig. 12. Influence of the stiffness of the soft soil on the coefficient G

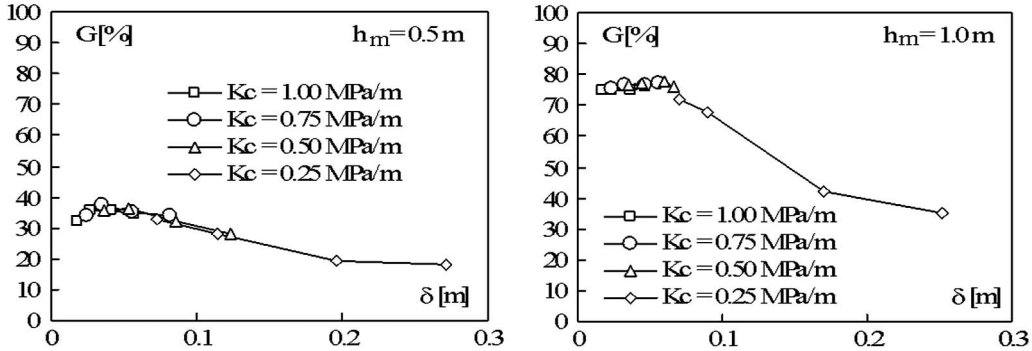

Fig. 13. Influence of the vertical settlement δ of the soft soil on the coefficient G

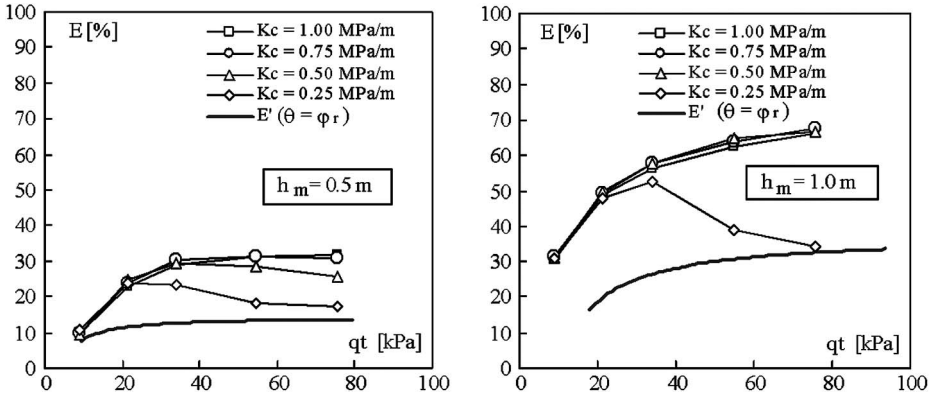

Fig. 15. Prediction of the efficiency E for high settlement of soft soil

Compared to Fig. 8, in which $K_c = 0.75$ MPa/m and $\theta = 44°$, the angle θ in Fig. 14 is smaller under large displacements, with a value of $\theta = 30°$ close to the residual friction angle φ_r. Consequently, the value of θ has to be assumed as equal to peak friction angle, as long as the soft soil settlement remains small enough (less than 0.05 m in the present case). For larger settlement of the soft soil, the angle θ decreases progressively until it reaches the value of residual friction angle φ_r (approximately 0.20 m settlement in the present case). Using $\theta = \varphi_r = 30.1°$ in Eq. (12), the estimated efficiency E' corresponds to the lowest limit obtained with the numerical values (Fig. 15). For the prediction of the load-transfer with Eq. (12), an iterative process must be used to find a value of θ compatible with the amplitude of the expected settlements. The value of θ should range between the peak friction angle and the residual friction angle of the granular material.

Influence of a Geosynthetic Sheet on Load-Transfer Mechanisms

The use of a geosynthetic sheet of reinforcement, inserted inside or at the base of the granular layer, is another means for increasing the redirection of the load to the piles. When geosynthetic sheets are used, the bending and large relative displacements of the granular layer are required to mobilize the tensile forces in the reinforcement sheet. Thus, thin granular layers seem more appropriate in this case; so h_m was set to 0.5 m in the numerical simulations. The geosynthetic sheet of reinforcement was placed at the base of the granular layer with two perpendicular directions of reinforcement with equal stiffness J. Values of the soft soil stiffness K_c ranging from 0.25 to 1.00 MPa/m were considered, as were two values of the geosynthetic stiffness: $J = 750$ kN/m and $J = 1{,}500$ kN/m.

The results of the numerical simulations are as follows:

1. The ability of the reinforced granular layer to redirect the overload to the piles G (Fig. 16), which can be compared with the nonreinforced cases (Fig. 12); and
2. The influence of the geosynthetic stiffness J on the settlements of the soft soil for a stiffness $K_c = 0.25$ MPa/m (Fig. 17).

Fig. 16 shows that the coefficient G is fairly constant for all the loading phases when a geosynthetic is used; this result differs from the case without geosynthetics, for which G decreased with the total load q_t for the softer subsoils.

In fact, with low overload, the small deformation of the granular layer does not enable the mobilization of significant tensile forces in the geosynthetic. Nevertheless, the action of the reinforcement is significant for greater displacements and contributes to the limita-

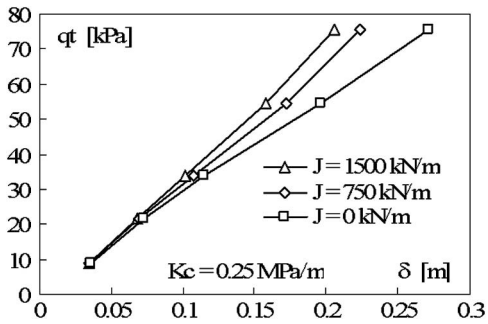

Fig. 17. Influence of the tensile stiffness of the geosynthetic on the vertical settlement of the soft soil

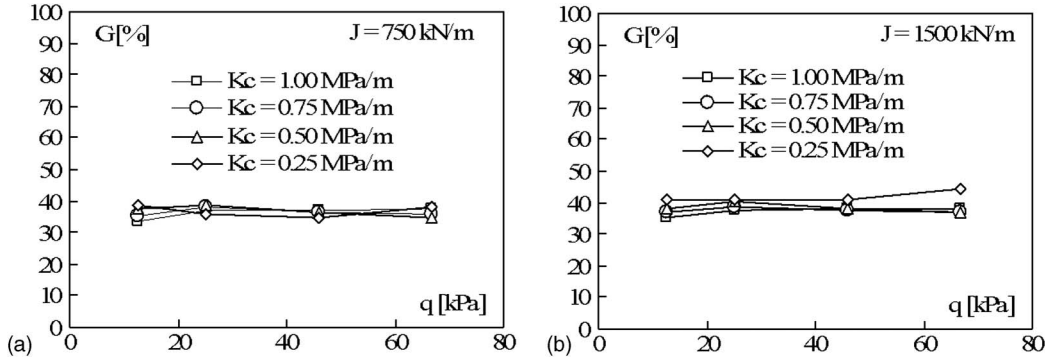

Fig. 16. Influence of the compressibility of the soft soil on the coefficient G ($h_m = 0.5$ m) with a geosynthetic sheet of stiffness (a) $J = 750$ kN/m; (b) $J = 1{,}500$ kN/m

tion of the vertical settlement (Fig. 17). The roles of the granular layer and the geosynthetic are complementary: the first acts for low settlements, and the second for extensive settlements. With the geometry studied, the coefficient G is fairly constant, depending on the vertical displacement of the soft soil. The predicted formulation of the efficiency, established previously without a geosynthetic, is still available in the case of a reinforced layer.

Case of Reinforcement Under a Slab

Soft soil reinforcement with rigid inclusions is also used as a foundation technique for buildings. Compared to the case under embankments, a concrete slab over the granular layer generates a vertical displacement condition. Consequently, specific load-transfer mechanisms appear, owing to the high bending characteristics of the slab.

In the numerical analysis, the concrete slab was modeled by a regular arrangement of spheres (Fig. 3) linked by bonds that are resistant to traction. The ratio of normal and tangential contact stiffnesses provided a global behavior of the assembly, similar to a shell element. The slab was embedded on all four sides (to represent the continuity of the slab). Figs. 18 and 19 show the evolution of E and G for $h_m = 0.5$ m and K_c ranging from 0.25 MPa/m to 1.0 MPa/m. The vertical displacements of the rigid slab, depending on the overload q, are given for different values of the soft soil stiffness K_c in Fig. 20.

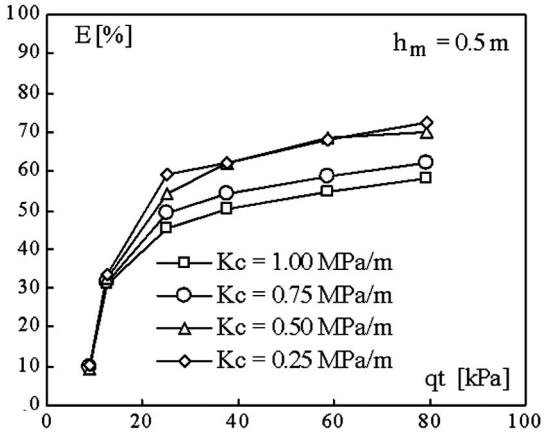

Fig. 18. Influence of the soft soil stiffness on the efficiency when a rigid slab is used

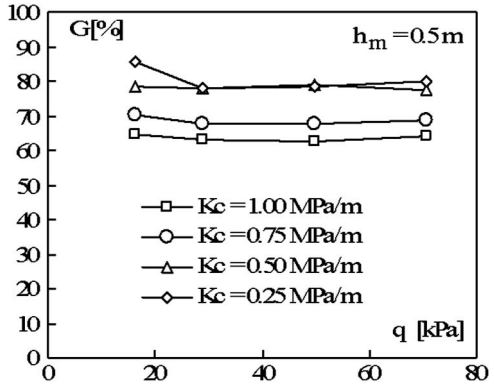

Fig. 19. Influence of the soft soil stiffness on coefficient G when a rigid slab is used

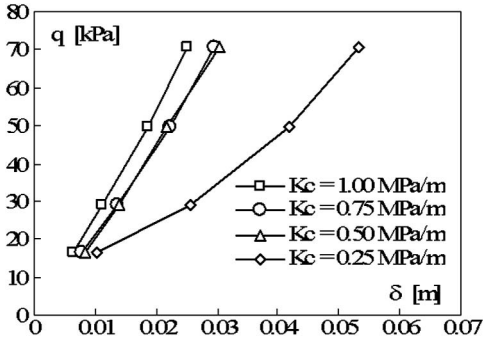

Fig. 20. Vertical settlements of the slab depending on the overload q for different values of K_c

These results show that, when a rigid slab is used, both the efficiency E and the ability of the load-transfer G to redirect the overload to the piles are much bigger than those obtained without a slab. The typical values of the efficiency of the reinforcement are as follows:

1. $E = 31.6\%$ and G approximately 38% under embankment; and
2. $E = 72.3\%$ and G approximately 80% under slab.

With a slab, as the stiffness of the soft soil decreases, Figs. 18 and 19 show that the efficiency of the load-transfer mechanisms increases, contrary to the case under embankment. In fact, based on the high bending rigidity of the concrete slab and the low stiffness of the compressible soil, part of the load is redirected to the network of piles through the columns of soil located over the inclusions. Consequently, an increase in the efficiency and the average vertical settlement is observed.

To compare mechanisms under embankment and under slab, the displacement fields of particles in the vertical cross-section A–A' are shown in Fig. 21 for the highest load and a soft soil stiffness K_c of 0.75 MPa/m. When a rigid slab is involved, the zone with very slight displacements is primarily restricted to the column located between the pile head and the concrete slab. In this case, the vertical settlement of the slab results from the vertical deformation of this part of the soil.

Comparing the results with Fig. 20 show a change in behavior for a very low value of K_c. To explain this, the stress states in the Mohr plane of the granular soil located directly above the piles are presented in Fig. 22 for different stages of the loading process and for $K_c = 0.25$ MPa/m and $K_c = 1.00$ MPa/m. For $K_c = 0.25$ MPa/m, the granular material has reached its maximal load capacity (peak strength). This is a result of both the high rate of the vertical loading σ_1 applied to the column of soil located directly over the pile and the low horizontal confining pressure σ_3 coming from the remaining part of the granular layer, and resulting from the high compressibility of the soft soil. Comparatively, the vertical load on the soft soil and consequently the horizontal confining pressure is greater for high values of K_c. On the contrary, the vertical load over the piles is not so great and consequently, vertical settlements are minor.

In conclusion, the mechanisms of load-transfer obtained when a rigid slab is used are rather different from those described without a slab. Owing to the high rigidity of the slab, the vertical settlements result from the deformation of the columns of soil located directly over the piles. This also depends on the rigidity of the load-transfer layer. The soft soil also has an influence on this, owing to its role in confining the soil directly above the piles. When maximal load capacity of the granular soil is reached for the softer soil, the settlement depends on both the mechanical properties of the soft soil

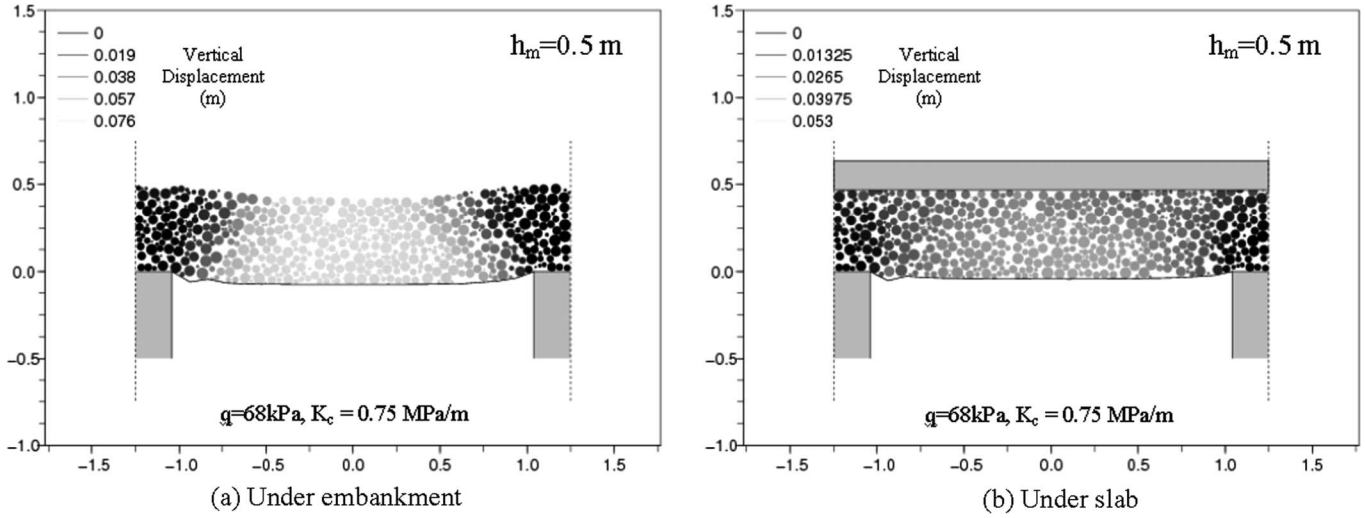

Fig. 21. Comparison of the particle displacements obtained with or without slab for the last stage of the loading process ($K_c = 0.75$ MPa/m): (a) under embankment; (b) under slab

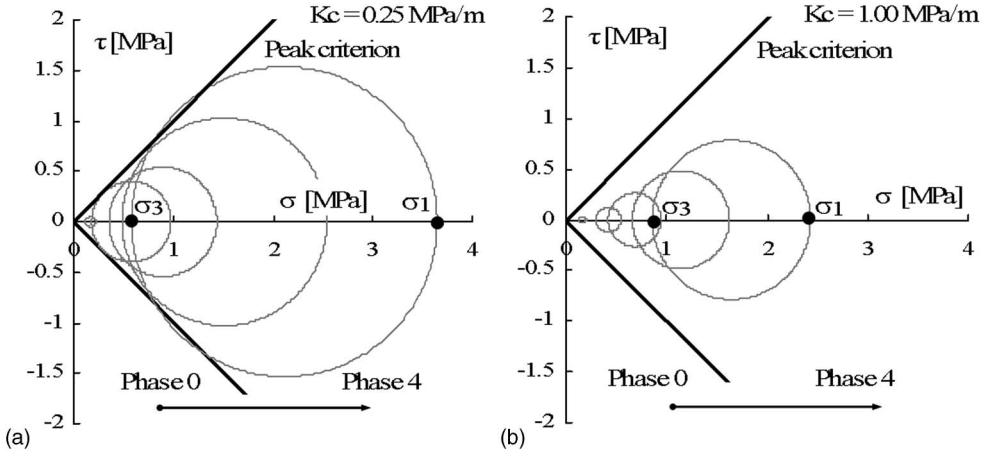

Fig. 22. Influence of the soft soil stiffness on the stress state in a column of soil sited over the piles, for different steps of the loading process (Phase 0 to 4): (a) $K_c = 0.25$ MPa/m; (b) $K_c = 1.0$ MPa/m

and the granular material (the stiffness and friction angle). Load transfers primarily occur in the columns of soil located directly over the piles: this implies a high concentration of vertical stresses on the slab over the piles, which needs to be considered in the design stage. This is true as long as the thickness of the granular layer is sufficiently low.

Conclusions

A numerical method coupling the discrete element method and finite-element method was used to study the load-transfer mechanism in a granular soil layer reinforced or nonreinforced by a geosynthetic sheet in the cases of soft soil reinforcement by rigid piles. A parametric study was carried out, based on realistic geometries and material properties defined in the framework of the French national project A.S.I.Ri, for several applications: reinforcement under embankments or under buildings. Thus, following the requirements of the national project and to reduce environmental impact, thicknesses of granular layers and coverage rates were deliberately considered to be lower than the recommendations in other methods.

Under embankments, the ability of the granular layer to redirect the load to the piles depends on its thickness and frictional characteristics. This mechanism takes place as soon as a slight settlement of the supporting soil is reached, and the load-transfer amplitude decreases as the vertical displacements of the granular layer increase.

The observation of the kinematics of the granular material was in good agreement with the prediction scheme of Carlsson, for which the granular material can be divided into two parts:

1. A zone of direct load-transfer sited over each pile, taking the shape of an inverted pyramid. This zone redirects its weight and the load it bears directly to the pile; and
2. A zone of no load-transfer composed of the remaining part of the granular layer. This part of the load-transfer layer transmits its weight and the loads it receives directly to the soft soil.

The primary difference between the mechanisms observed and the Carlsson description concerns the definition of the angle θ of the inverted pyramid zone. Whereas Carlsson recommended a value of $\theta = 15°$, the angle observed in the modeling was close to the friction characteristic of the granular material for extensive strain.

For low values of settlement, the prediction of the efficiency with Carlsson's description using the peak friction angle of the material gives satisfactory results. However, as the subsoil becomes softer, the settlements at the base of the granular layer increase and the angle θ of the pyramid-shaped zone decreases. This leads to a decrease in the efficiency of the load transfers. The variation of the angle θ is problematic for a reliable prediction of load transfers.

The insertion of a geosynthetic sheet at the base of the granular layer solved this problem: as soon as the settlements of the subsoil become too considerable, the geosynthetic sheet is activated and balances the mechanism in the granular layer.

Considering the case of a work under slab, this tendency is very different; this case found that the softer the subsoil, the more extensive the load-transfer to the piles. Nevertheless, the vertical settlement of the slab increases consecutively with the deformation of the column of soil sited over the pile, resulting from both an increase in the vertical load and a decrease in the confining pressure. In fact, for low values of the soft soil compressibility, the granular soil over the piles attains the failure criterion. The Carlsson description could not be recognized and consequently, as far as this parametric study is concerned, no prediction method can be easily proposed.

Notation

The following symbols are used in this paper:

a = size of the square pile (m);
d = diameter of load-transfer layer particles (m);
E = efficiency of the granular layer (-);
E' = predicted efficiency value of the granular layer (-);
E_0 = Young modulus (N/m^2);
E_{oed} = oedometric modulus of the soft subsoil (N/m^2);
F_p = resultant vertical force acting on the pile head (N);
F_z = resultant vertical force of the total load applied on the soft soil (N);
f_n = normal contact forces between particles (N);
f_t = tangential contact forces between particles (N);
G = ability of the granular load-transfer layer to redirect the overload to the piles (%);
h_c = equivalent height of the soft subsoil (m);
h_{ij} = overlap between contacting particles (m);
h_m = height of the granular load-transfer layer (m);
J = tensile stiffness of the geosynthetic sheet (N/m);
K_c = stiffness coefficient of the soft subsoil (N/m^3);
k_n = normal stiffness of the contact between particles (N/m);
k_t = tangential stiffness of the contact between particles (N/m);
k_{tg} = tangential stiffness of the contact between soil particles and geosynthetic sheets (N/m);
Q = resultant force of the overload applied on the load-transfer layer (N);
q = overload applied on granular layer (N/m^2);
q_t = stress equivalent to the total load applied on the soft soil (weight and overload) (N/m^2);
R_i = radius of particle i (m);
s = distance between the axes of the closest piles (m);
T = tensile force in the geosynthetic sheet (N/m);
U_0 = relative displacement from which the friction mobilization becomes maximum (m);
W = weight of the load-transfer layer (N);
W_p = weight of the zone of direct load transfers (N);
γ_d = density of the granular load-transfer layer (N/m^3);
δ = maximal settlement of the soft subsoil (m);
δu_t = incremental tangential displacement of contact points between particles (m);
ε = deformation of the geosynthetic sheet (-);
θ = orientation of the inverted pyramid-shaped zone of direct load-transfer (°);
μ = friction coefficient of the contact between particles (-);
ν = Poisson ratio (-);
σ_1 = vertical stress applied on the granular soil column sited over the pile (N/m^2);
σ_3 = horizontal confining pressure acting on the granular soil column sited over the pile (N/m^2);
φ_g = friction coefficient between soil particles and geosynthetic sheet elements (°);
φ_p = peak friction angle of the granular load-transfer layer (°); and
φ_r = residual friction angle of the granular load-transfer layer (°).

References

Abusharar, S. W., Zheng, J.-J., Chen, B.-G., and Yin, J.-H. (2009). "A simplified method for analysis of a piled embankment reinforced with geosynthetics." *Geotext. Geomembr.*, 27, 39–52.

Allen, M. P., and Tildesley, D. J. (1994). *Computer simulation of liquids*, Oxford Science Publications, Oxford, UK.

Briançon, L. (2007). *A.S.I.RI.—Tranche 1—Thème 1: Rapport final*. Rapport technique *1-07-1-02*, Conservatoire National des Arts et Métiers, Paris.

British Standards Institution. (1995). "Design of embankments with reinforced soil foundation on poor ground." *British Standard 8006: Code of practice for strengthened/reinforced soils and other fills*, 80–121.

Carlsson, B. (1987). *Armerad jord beräkningsprinciper för vertikala väggar, branta slänter, bankar på lös undergrund, bankra på pålar*, Terrateam AB, Linköping, Sweden.

Chareyre, B., and Villard, P. (2005). "Dynamic spar elements and DEM in two dimensions for the modelling of soil-inclusion problems." *J. Eng. Mech.*, 131(7), 689–698.

Chevalier, B., Combe, G., and Villard, P. (2007). "Study of the mechanical behavior of heterogeneous granular materials by means of distinct element method." *Bulletin des Laboratoires des Ponts et Chaussées*, 268/269, 105–128.

Chevalier, B. (2008). "Etudes expérimentale et numérique des transferts de charge dans les matériaux granulaires: Application aux renforcements de sols par inclusions rigides." Ph.D. thesis, Université Joseph Fourier, Grenoble, France.

Chevalier, B., Combe, G., and Villard, P. (2008). "Experimental and numerical studies of load transfers and arching effect." *Proc., 12th Int. Conf. of the Int. Association for Computer and Advances in Geomechanics (IACMAG), Goa, India*, IACMAG, Tucson, AZ, 273–280.

Combarieu, O. (1988). "Amélioration de sols par inclusions rigides verticales—Application à l'édification de remblais sur sols médiocres." *Rev. Fr. Geotech.*, 44, 57–79.

Combarieu, O. (1990). "Fondations superficielles sur sol amélioré par inclusions rigides verticales." *Rev. Fr. Geotech.*, 53, 33–44.

Combe, G. (2002). "Mécanique des matériaux granulaires et origines microscopiques de la déformation." *Etudes et recherches du Laboratoire Central des Ponts et Chaussées*, LCPC, Paris.

Cundall, P. A., and Strack, O. D. L. (1979). "A discrete numerical model for granular assemblies." *Geotechnique*, 29(1), 47–65.

Deutsche Gesellschaft für Geotechnik (2004). *EBGEO: Empfehlungen für Bewehrungen aus GEOkunststoffen: Bewehrte Erdkörper auf punkt-oder linienförmigen Traggliedern*, Desutsche Gesellschatf für Geotechnik, Essen, Germany.

Gilbert, R. B., and Byrne, R. J. (1996). "Strain-softening behavior of waste containment system interfaces." *Geosynth. Int.*, 3(2), 181–203.

Gourc, J. P., and Villard, P. (2000). "Reinforcement by membrane effect: Application to embankments on soil liable to subsidence." *Proc., 2nd Asian Geosynthetics Conf.: Geosynthetics ASIA 2000, Kuala Lumpur, Malaysia*, 1, Int. Geosynthetics Society, West Palm Beach, FL, 55–72.

Han, J. and Gabr, M. A. (2002). "A numerical study of load transfer mechanisms in geosynthetic reinforced and pile supported embankments over soft soil." *J. Geotech. Geoenviron. Eng.*, 128(1), 44–53.

Hewlett, W., and Randolph, M. A. (1988). "Analysis of piled embankments." *Ground Eng.*, 21(3), 12–18.

Kempfert, H. G., Stadel, M., and Zaeske, D. (1997). "Berechnung von geokunststoffbewerten Tragschichten über Pfahlelementen." *Bautechnik*, 74(12), 818–825.

Kuwano, R., and Jardine, R. J. (2002). "On the applicability of cross-anisotropic elasticity to granular materials at very small strains." *Géotechnique*, 52, 727–749.

Øiseth, E., and Busklein, J. O. (2001). "Rembank—User's manual version 2.0." *SINTEF Rep. STF22 F01133/F01134*, SINTEF, Trondheim, Norway.

Pasqualini, E., Roccato, M., and Sani, D. (1993). "Shear resistance at the interfaces of composite liners." *Proc., 4th Int. Landfill Symp.: Sardinia 93, Cagliari, Italy*, CISA, Padova, Italy, 1457–1471.

Reddy, K. R., Kosgi, S., and Motan, E. S. (1996). "Interface shear behavior of landfill composite liner systems: A finite element analysis." *Geosynth. Int.*, 3(2), 247–275.

Russel, D., and Pierpoint, N. (1997). "An assessment of design methods for piled embankments." *Ground Eng.*, 30(11), 39–44.

Schäfer, S., Dippel, S., and Wolf, D. (1996). "Forces schemes in simulations of granular materials." *J. Phys. I (France)*, 6(1), 5–20.

Svanø, G., Ilstad, T., Eiksund, G., and Watn, A. A. (2000). "Alternative calculation principle for design of piled embankments with base reinforcement." *Proc., 4th Conf. of the GIGS, Finland*, Finnish Geotechnical Society, Helsinki, Finland.

Terzaghi, K. (1943). *Theoretical soil mechanics*, Wiley, New York.

Villard, P. (1996). "Modelling of interface problems by the finite element method with considerable displacements." *Comput. Geotech.*, 19(1), 23–45.

Villard, P., Chevalier, B., Le Hello, B., and Combe, G. (2009). "Coupling between finite and discrete element methods for the modelling of earth structures reinforced by geosynthetic." *Comput. Geotech.*, 36(5), 709–717.

Villard, P., and Giraud, H. (1998). "Three-dimensional modelling of the behaviour of geotextile sheets as membrane." *Textile research Journal : publication of Textile Research Institute, Inc and the Textile Foundation*, 68, 797–806.

Villard, P., Gourc, J. P., and Giraud, H. (2000). "A geosynthetic reinforcement solution to prevent the formation of localized sinkholes." *Can. Geotech. J.*, 37, 987–999.

Yun-Min, C., Wei-Ping, C., and Ren-Peng, C. (2008). "An experimental investigation of soil arching within basal reinforced and unreinforced piled embankments." *Geotext. Geomembr.*, 26, 164–174.